Transactions of the Korean Nuclear Society Spring Meeting
Jeju, Korea, May 12-13, 2016

Effects of corrosion and precipitates on mechanical properties in the ferritic/martensitic steel cladding under ultra-long cycle fast reactor environment at 650°C

Tae Yong Kim[a], Sang Hun Shin[b], Jeonghyeon Lee[a] and Ji Hyun Kim[a*]
[a] *School of Mechanical and Nuclear Engineering, Ulsan National Institute of Science and Technology (UNIST), Ulju-gun, Ulsan 44919, Republic of Korea*
[b] *Korea Atomic Energy Research Institute (KAERI), Yuseong-gu, Daejeon 34057, Republic of Korea*
[*] *Corresponding author: kimjh@unist.ac.kr*

1. Introduction

Liquid sodium used with coolant of Ultra-long Cycle Fast Reactor(UCFR) has thermal efficiency by good thermal conductivity (87.1 W/m·K) and specific heat (1.38kJ/kg). The low viscosity and wide range of liquid temperature (97.8~883 °C) which give large margin for reactor design can provide safe operation. Ferrite martensitic steels which are used as one of cladding and structure materials in UCFR, have high creep strength at 600~650°C, low expansion coefficient, and dimensional stability with irradiation-induced void swelling in circumstance of fast neutrons compared to austenitic stainless steel [1-3]. However, as exposed to high temperature liquid sodium during the design life time (30 to 60 years), the surface of ferritic/martensitic steel experienced Cr-depletion and decarburization by dissolution of components into sodium and formed oxidations by reacting with sodium [4]. This changes chemical compositions of inter-surface and effects on behavior of precipitations. $NaCrO_2$ which is ternary sodium compound occurs intergranular corrosion resulting in thickness reduction. This change can cause a degradation of mechanical strength of structure material of UCFR. Therefore, we should consider long-term compatibility with sodium and study about life prediction.

The research about ferritic/martensitic steel on effects of long term exposure in liquid sodium at 650 °C, 20ppm oxygen includes weight loss of test material (Gr. 92) by corrosion and mechanism about nucleation and growth of precipitates like Laves-phase in bulk. There are many changes such as segregation of component to nucleate precipitates, affecting into microstructural evolution of the steel. Therefore, the thermochemical reaction research to predict behavior about precipitates should be performed.

In a specific procedure, the micro-structure and the surface phenomenon of ferritic/martensitic steels (Gr. 92) that are exposed to liquid sodium at 650°C, 20 ppm oxygen and aged in high pure Argon gas environment to express bulk have been investigated by using scanning electron microscope (SEM) and transmission electron microscope (TEM) [5-6].

2. Experimental

The test material in this study is ASTM A182 Gr.92 steel, which contains approximately 9 wt. % of chromium and 2 wt. % of tungsten. Chemical composition of this material is shown in Table. 1. Tub of Gr.92 were manufactured by hot extrusion and multiple passes of cold drawing. The tubes were normalized at 1080 °C for 6 min and tempered at 800°C for 6 min so as to develop a tempered martensite structure [7].

Table I. Chemical compositions in wt.% of Gr.92 alloy (wt.%).

C	Si	Mn	Cr	Ni	Mo	W
0.087	0.21	0.41	8.69	0.13	0.38	1.62
V	Nb	Cu	N	B	P	S
0.18	0.07	0.10	0.046	0.002	0.012	0.002

There are two kind of Gr. 92 cladding tubes. Some were exposed to liquid sodium at 650 °C, saturated oxygen (3871 ppm calculated by [8]) for 1583 hours. The others were exposed to 650 °C liquid sodium at initially 20 ppm oxygen for 1512 h and then at saturated for 1583 hours, totally 3095 hours. As a comparative control to test the effect of sodium, other Gr. 92 cladding tubes were encapsulated in a 99.99 % pure Ar environment, and then kept in a 650 °C muffle furnace for 1601 hours or 2973 hours. The test loop is made of 316 stainless steel. In order to observe cross section of specimens, they were cut with and treated with mounting. And then, specimen cross sections were polished with 0.04 μm alumina particles and etched with a mixed acid solution (93 vol. % water, 5 vol. % nitric acid and 2 vol. % fluoric acid) to observe apparent cross sections.

Compared with effects of sodium environment, Ar-gas aging experiment is accomplished. Therefore, effects of sodium are evaluated by analyzing thickness reduction with formation of oxidation composed with sodium and dissolution of elements like Cr and C into sodium, resulting in depleted zone and precipitates free zone at inter surface.

The final goal of this experiment is analysis of inter surface and precipitation of steels. And mechanical properties changes by sodium environment are related with corrosion, dissolution and precipitation hardening.

3. Results and Discussions

3.1 SEM analysis

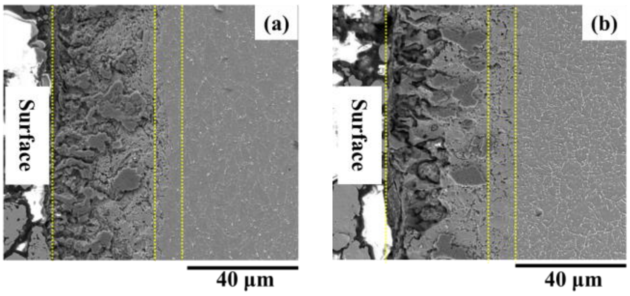

Figure. 1. SEM images of cross-section of specimen after exposure to 650℃ sodium for (a) 1583 h and (b) 3095 h [7].

Figure 1 (a) and (b) show cross-section of specimens which exposed to 650 ℃ sodium for 1583 hours with saturated dissolved oxygen and for 3095 hours (1583 hours with 20 ppm, after that, with saturated). Oxidations are found from Fig. 1. In Fig. 1, eluted chromium reacting with sodium forms 10~20 μm sized oxides on the surface up to 40 μm. In Fig. 1, some little oxides were formed on the same region. From the preceding research conducted by Shin et al. $NaCrO_2$ oxide is the most stable sodium oxide known as ternary compound. Intergranular corrosion occurred through the sodium oxide region about 40 μm in both specimens. But in Fig. 1 (b), after exposed to sodium more than before the more pores can be found, and corrosion occurs more severe. From EPMA X-ray mapping, it can be found Cr depletion and decarburization from 40 μm to 50 μm section.

In sodium environment, thickness reduction of ferritic/martensitic steel occurred, because both the elements elution to sodium and formation of sodium oxide induce corrosion. The thickness reduction rate of Gr.92 at the loop of sodium in 20 ppm and 650 ℃ is about 6.76 μm/yr [9]. Therefore, it can be calculated that the thickness of specimen exposed to 20ppm sodium during 1583h decreases about 1.2 μm. To figure out the decrease of thickness during remained 1512 hours after 1583 hours in 3871 ppm saturated oxygen environment, the relation formula between dissolved oxygen and corrosion speed is needed. According to H.Y. Borgborgs et al. corrosion speed formula related with dissolved oxygen in 600-700 ℃ is followed.

$$\mathrm{Log}(k)=-1.662+0.922\log(C) \tag{1}$$

'k' term means the corrosion speed of the specimen, and 'C' means the amount of dissolved oxygen in liquid sodium.

Based on the equation (1) the change of corrosion rate in liquid sodium of 3871 ppm and 20 ppm dissolved oxygen is followed.

$$\mathrm{Log}(k_{3871}/k_{20})=0.922\log(C_{3871}/C_{20}) \tag{2}$$

From this K_{3871} and K_{20} are the corrosion speed of 3871 ppm and 20 ppm respectively, C_{3871} and C_{20} means the amount of dissolved oxygen of 3871 ppm and 20 ppm respectively. According to the relationship, the corrosion rate of 3871 ppm dissolved oxygen with respect to the corrosion rate of 20 ppm dissolved oxygen is followed.

$$K_{3871}/K_{20}=128.36 \tag{3}$$

So, the corrosion rate of Gr.92 in sodium of 3871 ppm dissolved oxygen is 867 μm/yr and the total reductions of thickness for 1583 hours and 3095 hours are 156.8μm and 158μm, respectively.

The designed maximum value of dissolved oxygen in UCFR is 10 ppm, and the corrosion speed is 3.568 μm/yr earned from the formula. During the minimum life span of UCFR, 30 years, the thickness decreases about 107 μm. Suppose the thickness of cladding as 570 μm, this reduction equals to the 18.8 % decrease in thickness and 19.07 % decrease in area. Thus, if there is no degradation of mechanical strength caused by aging effect, the tolerance of load of initial cladding should be higher than real load at least 23.6 %.

If the oxygen in sodium saturates in the case of accident, the corrosion rate will be 868 μm/yr, then 45 days are needed to reduce the thickness up to 107 μm. So, it is hard to break secondary accident caused by thickness reduction of cladding in case of accident.

Fig. 2 (a) and (b) is SEM image of cross section of Gr.92 specimen thermally aged during 1601 hours and 2973 hours in 650 ℃ Ar-gas environment. There are no forming oxide and intergranular corrosion unlike sodium environment. There is no change also in the size of sub grain regarding to aging time.

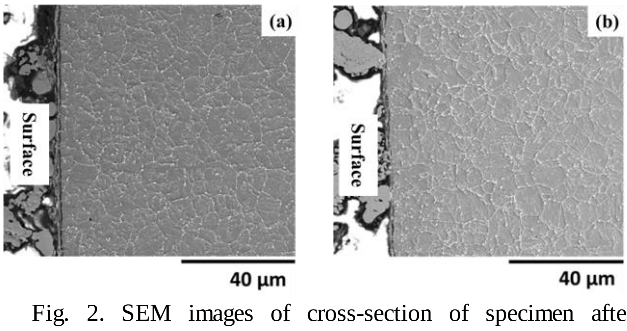

Fig. 2. SEM images of cross-section of specimen after exposure to 650 ℃ Ar-gas for (a) 1601 h and (b) 2973 h [7].

3.2 TEM analysis

During HR-TEM analysis on FIB samples, a few points in the steel matrix (not precipitates) were analyzed by EDS. In the matrix, Cr-content varies from 4.87 wt. % to 6.24 wt. % at the interface between the Cr-depleted zone and the bulk steel matrix from surface in the sodium exposed sample, and from 5.9 wt. % to 7.74 wt. % in the argon-exposed sample [7].

The amount of precipitations of specimens exposed to sodium is more than that of specimens exposed to Ar-gas. Using TEM images of carbon extraction replicas, count and diameter of precipitations are charted at Table II and III.

Table II: Count of precipitations [7]

	Sodium	Ar-gas
About 1600 h	140	182
About 3000 h	104	152

Table III: Diameter of precipitations [7]

	Sodium	Ar-gas
About 1600 h	113	143
About 3000 h	218	171

In the sodium exposed sample, precipitates represent mainly $M_{23}C_6$ carbide. $M_{23}C_6$ is complex compound composed with Cr, Fe, W, Mo and C. This precipitation is formed at prior austenite grain boundary, subgrain or lath boundary. Laves phase observed from the bulk steel matrix in Na-exposed specimen and from the Ar-exposed specimen.

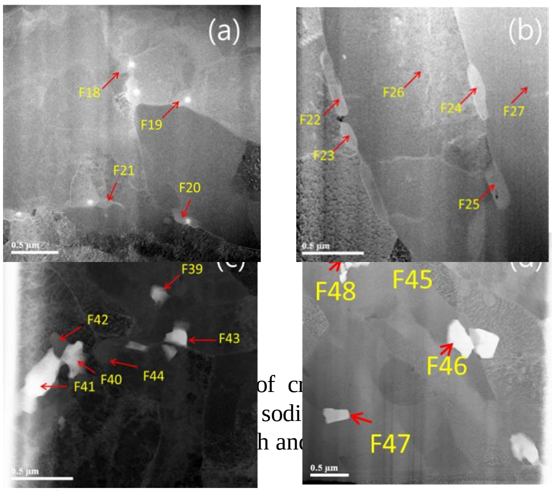

of cr after
sodi 3095
h an

After 1600 hours, specimens exposed to sodium have a few of $M_{23}C_6$ and Laves phase due to depletion of Cr and C which are components of two precipitations. Therefore, the number and diameter of precipitations of the specimens is less than that exposed to Ar-gas environment. By coarsening of precipitations, their volume increases but the number of them decreases. However, precipitations volume of specimen exposed to sodium rapidly increases, but volume increase of that exposed to Ar-gas is relatively small. Reason of that is formation of Laves phase which nucleate slowly. New small laves phase effects on small mean diameter [10].

Through the J-MatPro thermodynamic program, composition of laves phase is 9.52 at. % Cr, 4.57 at. % Mo, 28.68at. % W, 56.17 at. % Fe, 0.77 at. %Si and described with $(Fe,Cr)_2W$ at Gr.92. The chemical composition of the Laves phase particles is not affected by stress [10]. Also, slow diffusion rate of Si which is component of Laves phase retards that laves phase reaches thermal equilibrium state over 140,000 hours [10]. Therefore, the number of density and area fraction of laves phase continuously increases.

When Gr.92 is exposed to liquid sodium for 2333 hours, micro-hardness decreases with 208 VHN from 256 VHN, because of coarsening, formation of sub-grain and annealing of lath structure [4]. Micro-hardness is inverse proportional to plastic deformation. So, high hard material hinders motion of dislocation. Since strength also increase as much as hindering dislocation, there is linear relationship between hardness and strength. Therefore, As-receive Gr.92 has 618 MPa at real temperature. After exposed to sodium, strength is calculated with 468 MPa [9]. Moreover, decarburization and Cr-depletion at inter-surface decrease total mechanical properties. Therefore, the strength of Gr.92 exposed to sodium is decreased with 464.2 MPa [9]. Strength of Cr-depleted and decarburization region can be calculated with next equation.

$$\sigma_t = \frac{t_m}{t_0}\sigma_m + \frac{t_{depleted}}{t_0}\sigma_{depleted} \qquad (4)$$

'σ_t' is total strength of cladding, 't_m' is thickness of bulk, 't_0' is final thickness of cladding, 'σ_m' is strength of bulk, '$t_{depleted}$' is thickness of depleted zone and '$\sigma_{depleted}$' is strength of depleted zone. So, the strength of depleted zone is calculated with 416.2 MPa. Strength of bulk of metal is 12 % higher than strength of depleted zone.

There are two factors affecting on solid solution hardening and precipitation hardening. In precipitation hardening, Precipitations act on grain depending on size and distribution of precipitations [11].

$$F = \pi r \gamma \sin 2\theta \qquad (5)$$
$$P = F \cdot n_s \qquad (6)$$

'F' is force exerted by a single precipitation at boundary, 'r' is radius of precipitation, 'γ' is surface energy, 'n_s' is number of precipitations per unit area, 'P' is pressure exerted by precipitations at boundary.

Although precipitations exposed to sodium experience more coarsening than for 1600 hour, increase of size strengthen precipitation hardening effect with 59 %, neglecting γ and θ, through Table I and II. On the other hands, decrease of number density of precipitation by coarsening makes precipitation hardening effect weaken 0.1 %. Nevertheless, precipitation hardening effect at Ar-gas environment is 81 % and 12 % larger than at sodium environment for 1600 hours and 3000 hours, respectively.

Compared with experiment values, depleted zone is influenced by reduction of solid solution resulting in decrease of strength, but the strength recovers by precipitation hardening with time. However, decreasing strength of specimens exposed to Ar-gas has little dependence on coarsening of precipitations without effect of reduced solid solution.

According to preceding research about creep rate, Laves-phase which is fine precipitation decreases creep rate. Therefore, creep rate decrease as increasing the number of precipitation. Because creep rate also decreases when there are many particles which hind a movement of dislocation, decreasing creep strength means increasing strength. Thus, at Ar-gas environment, strength increase with many precipitations. However, increasing precipitation rate of Laves-phase at 650 ℃ results in the large coarsening of Laves-phase [12]. Although there are coarsening at Ar-gas environments, many precipitation is still observed. This means that it is not sufficient time to reach equilibrium state of Laves-phase at 650 ℃. Computed kinetics of tungsten precipitation in P92 steel shows that equilibrium state can be reached after 4000 hours [13]. So, this research studied under 4000 hours shows that precipitation hardening is dependent rather than coarsening of Laves-phase. However, after 4000 hours, effect of coarsening of Laves-phase is predicted to reduce strength of cladding. For durability of cladding operated during long hours, a cladding material exposed to sodium for 4000 hours or more is needed.

4. Conclusions

When Ferritic/martensitic steels are exposed to 650 ℃ liquid sodium for 1583 hours and 3095 hours, mechanical properties of materials were analyzed quantitatively.

After experiment, $NaCrO_2$ oxidation was formed on the surface of Gr.92. According to dissolved oxygen at sodium, surface corrosion rate is different. At 10 ppm oxygen designed oxygen value for UCFR, there is 107μm thickness reduction for 30 years. Thus, if there is no degradation of mechanical strength caused by aging effect, the tolerance of load of initial cladding should be higher than real load at least 23.6 %.

Compared to specimens exposed to Ar-gas environment, Specimen which solutions are leaded into sodium has degradation of strength by reduction of solution hardening. However, the strength recovers with precipitation hardening with time. On the other hands, specimen exposed to Ar-gas environment, the strength is decreased by coarsening of precipitations.

ACKNOWLDEGEMENT

This work was supported by NRF (National Research Foundation of Korea) Grant funded by the Korean Government (2015M2B2A4031824).

REFERENCES

[1] S.H. Shin, J.J. Kim, J.A. Jung, K.J. Choi and J.H. Kim, Development of experimental system for materials compatibility test for ultra-long cycle fast reactor (UCFR), NFSM, American Nuclear Society, 2012, Chicago, IL.

[2] S. H. Shin et al., Corrosion behavior and microstructural evolution of ASTM A182 Grade 92 steel in liquid sodium at 650C, Corrosion Science, Vol.97, pp.172-182, 2015.

[3] S. H. Shin et al., A study on corrosion behavior of austenitic stainless steel in liquid metals at high temperature, Journal of Nuclear Materials, Vol.422, pp.92-102, 2012.

[4] H. L. klueh and D. R. Harries, High-Chromium Ferritic and Martensitic Steels for Nuclear Applications, American Society for Testing and Materials, pp.33, 2001.

[5] S. H. Shin et al., Model of liquid gallium corrosion with austenitic stainless steel at a high temperature, Journal of Nuclear Materials, Vol.450, pp.314-321, 2014.

[6] S. W. Lee, S. D. Park, S. Kang, S. H. Shin, J. H. Kim and I. C. Bang, Feasibility study on molten gallium with suspended nanoparticles for nuclear coolant applications, Nuclear Engineering and Design, Vol.247, pp.147-159, 2012.

[7] S.H. Shin, J.H. Kim and J.H. Kim, Effect of Aging ASTM A182 Grade 92 Steel on Corrosion Behavior and Microstructural evolution in Liquid Sodium at 650℃, Corrosion science, Vol.97, pp.172-182, 2015.

[8] R. L. Eichelberger, THE SOLUBILITY OF OXYGEN IN LIQUID SODIUM : A RECOMMENDED EXPRESSION, A DIVISON OF NORTH AMERICAN ROCKWELL CORPORATION, pp.1-21, Nov.1, 1968.

[9] J. H. Kim, J. M. Kim, S. H. Kim, and C. B. Lee, Microstructural and Mechanical Property Evaluation of the Ferritic-Martensitic Steel under Liquid Sodium Environment, SFR Fuel Cladding Deveopment, Korea

Atomic Energy Research Institute, Kor. J. Met. Mater., Vol.48, pp.914-921.

[10] A. Aghajani, F. Richter, C. Somsen, S. G. Fries, I. Steinbach and G. Eggeler, On the formation and growth of Mo-rich Laves phase particles during long-term creep of a 12% chromium tempered martensite ferritic steel, Scripta Materialia, Vol.61, pp.1068-1071, 2009.

[11] D. A. Porter et al., Phase transformations in metals and alloys – third edition, pp.145, 2009.

[12] Fujio Abe, Creep rates and strengthening mechanisms in tungsten-strengthened 9Cr steels, Materials Science and Engineering, pp.770-773, 2001.

[13] Ronald L. Klueh and Donald R. Harries, High-Chromium Ferritic and Martensitic Steels for Nuclear Applications, ASTM, pp.42, 2001.